

Eigenvectors from Eigenvalues Sparse Principal Component Analysis (EESPCA)

H. Robert Frost¹

¹*Department of Biomedical Data Science
Geisel School of Medicine
Dartmouth College
Hanover, NH 03755, USA
rob.frost@dartmouth.edu*

Abstract

We present a novel technique for sparse principal component analysis. This method, named Eigenvectors from Eigenvalues Sparse Principal Component Analysis (EESPCA), is based on the recently rediscovered formula for computing normed, squared eigenvector loadings of a Hermitian matrix from the eigenvalues of the full matrix and associated sub-matrices. Relative to the state-of-the-art sparse PCA methods of Witten et al., Yuan & Zhang and Tan et al., the EESPCA technique offers a two-orders-of-magnitude improvement in computational speed, does not require estimation of tuning parameters via cross-validation, and can more accurately identify true zero principal component loadings across a range of data matrix sizes and covariance structures. Importantly, EESPCA achieves these performance benefits while maintaining a reconstruction error close to that generated by these other approaches. EESPCA is a practical and effective technique for sparse PCA with particular relevance to computationally demanding statistical problems such as the analysis of high-dimensional data sets or application of statistical techniques like resampling that involve the repeated calculation of sparse PCs.

Keywords: principal component analysis, sparse principal component analysis, sparse eigenvalue decomposition, eigenvector-eigenvalue identity

1 Introduction

1.1 Principal component analysis (PCA)

PCA is a widely used statistical technique that was developed independently by Karl Pearson (Pearson, 1901) and Harold Hotelling (Hotelling, 1933) in the early part of the 20th century. PCA performs a linear transformation of multivariate data into a new set of variables, the principal components (PCs), that are linear combinations of the original variables, are uncorrelated and have sequentially maximum variance (Jolliffe, 2002). PCA can be equivalently defined by the set of uncorrelated vectors that provide the best low-rank matrix approximation, in a least squares sense. The solution to PCA is given by the eigenvalue decomposition of the sample covariance matrix with the variance of the PCs specified by the eigenvalues and the PC directions defined by the eigenvectors.

Because PCA is defined in terms of the eigenvectors and eigenvalues of the sample covariance matrix, it is related to a wide range of matrix analysis methods and multivariate statistical techniques with an extremely large number of applications (Jolliffe, 2002; Jolliffe and Cadima, 2016).

Although most commonly used for unsupervised linear dimensionality reduction and visualization, PCA has been successfully applied to statistical problems including regression (e.g., principal components regression (Hastie *et al.*, 2009)), clustering (e.g., use of PCs as input for clustering methods (Hafemeister and Satija, 2019; Waltman and van Eck, 2013)), and non-linear dimensionality reduction (e.g., seed directions for non-linear methods (McInnes *et al.*, 2018)). In the biomedical domain, PCA has been extensively employed for the analysis of genomic data including measures of DNA variation, DNA methylation, RNA expression and protein abundance (Ma and Dai, 2011). Common features of these datasets, and the motivation for eigenvalue decomposition methods, are the high dimensionality of the feature space (i.e., from thousands to over one million), comparatively low sample size (i.e., $p \gg n$) and significant collinearity between the features. The most common uses of PCA with genomic data involve dimensionality reduction for visualization or clustering (Stuart *et al.*, 2019), with population genetics an important use case (Patterson *et al.*, 2006). PCA has also been used as the basis for feature selection (Lu *et al.*, 2011), and gene clustering (Kluger *et al.*, 2003). More recent applications include gene set enrichment of bulk or single cell gene expression data (Fan *et al.*, 2016; Tomfohr *et al.*, 2005).

1.2 Mathematical notation for PCA

Let \mathbf{X} be an $n \times p$ matrix that holds n independent samples drawn from a p -dimensional joint distribution with population covariance matrix Σ . Without loss of generality, we can assume the columns of \mathbf{X} are mean-centered. The unbiased sample covariance matrix is therefore given by $\hat{\Sigma} = 1/(n-1)\mathbf{X}^T\mathbf{X}$. PCA can be performed via the direct eigenvalue decomposition of $\hat{\Sigma}$ with the eigenvalues λ_i equal to the PC variances and the eigenvectors \mathbf{v}_i equal to the PC loadings. For computational reasons, PCA is more commonly performed via the singular value decomposition (SVD) of \mathbf{X} : $\mathbf{X} = \mathbf{U}\mathbf{D}\mathbf{V}^T$, where \mathbf{U} and \mathbf{V} are both orthonormal matrices (i.e., $\mathbf{U}^T\mathbf{U} = \mathbf{V}^T\mathbf{V} = \mathbf{I}$), the columns of \mathbf{V} represent the PC loading vectors, the entries d_i in the diagonal matrix \mathbf{D} , arranged in decreasing order, are proportional to the square roots of the PC variances ($d_i = (n-1)\sqrt{\lambda_i}$) and the columns of $\mathbf{U}\mathbf{D}$ are the principal components. Consistent with the optimal low-rank matrix approximation property of PCA, the first r components of the SVD minimize the squared Frobenius norm between the original \mathbf{X} and a rank r reconstructed version of \mathbf{X} . Specifically, if \mathbf{U}_r , \mathbf{D}_r and \mathbf{V}_r hold the first r columns of \mathbf{U} , \mathbf{D} and \mathbf{V} , $\hat{\mathbf{X}}_r = \mathbf{U}_r\mathbf{D}_r\mathbf{V}_r^T$ is the SVD rank r reconstruction of \mathbf{X} , which minimizes $\|\mathbf{X} - \hat{\mathbf{X}}_r\|_F^2$ for all possible rank r reconstructions.

In the remainder of the manuscript we will use $\|\mathbf{x}\|_0$ to refer to the l_0 norm of vector \mathbf{x} (i.e., number of non-zero values), $\|\mathbf{x}\|_2$ to refer to the Euclidean or l_2 norm, $(\mathbf{x})_i$ to refer to element i of vector \mathbf{x} , $|\mathbf{x}|_n$ to refer to the vector \mathbf{x} normalized to unit length (i.e., $\mathbf{x}/\|\mathbf{x}\|_2$), and $\mathbf{x} \odot \mathbf{y}$ to refer to the element-wise multiplication of vectors \mathbf{x} and \mathbf{y} . Additional mathematical notation is defined when first used.

1.3 Running example

To help illustrate the concepts discussed in this paper, we introduce a simple example data set based on a 10-dimensional multivariate normal (MVN) distribution. The R logic needed to reproduce all of the results for this example can be found at <http://www.dartmouth.edu/~hrfrost/EESPCA>. The population mean is set to the zero vector, $\boldsymbol{\mu} = (0, 0, 0, 0, 0, 0, 0, 0, 0, 0)$, and the population covariance matrix is given a two block covariance structure with a covariance of 0.5 among the first four variables and between the last two variables, and a covariance of 0 among all other variables. All population variances are set to one, which aligns with the common practice of performing PCA after standardization. For this Σ , the first population PC has equal non-zero loadings for just the

first four variables and the second population PC has equal non-zero loadings for just the last two variables. If the matrix \mathbf{V} holds the population PC loadings, the first two columns are:

$$\mathbf{V}[:, (\mathbf{1}, \mathbf{2})]^T = \begin{bmatrix} -0.5 & -0.5 & -0.5 & -0.5 & 0 & 0 & 0 & 0 & 0 & 0 \\ 0 & 0 & 0 & 0 & 0 & 0 & 0 & 0 & 0.7071068 & 0.7071068 \end{bmatrix}$$

The variances of these population PCs are $\boldsymbol{\lambda} = (2.5, 1.5)$.

For an example set of 100 independent samples drawn from this MVN distribution, the loadings of the first two sample PCs (rounded to three decimal places) are:

$$\hat{\mathbf{V}}[:, (\mathbf{1}, \mathbf{2})]^T = \begin{bmatrix} -0.541 & -0.446 & -0.506 & -0.496 & -0.033 & 0.022 & 0.001 & -0.023 & -0.049 & -0.052 \\ 0.113 & -0.085 & -0.055 & -0.126 & 0.156 & -0.048 & 0.002 & -0.221 & 0.724 & 0.600 \end{bmatrix}$$

The variances of the first two sample PCs (again rounded to three decimal places) are $\hat{\boldsymbol{\lambda}} = (3.393, 1.521)$. The minimum rank 2 reconstruction for this case (computed as the squared Frobenius norm of the residual matrix) is 597.531.

1.4 Sparse PCA

As demonstrated by the simple example above, all variables typically make a non-zero contribution to each sample PC even when the data follows a statistical model with sparse population PCs. This property makes interpretation of the PCs challenging, especially when the underlying data is high dimensional. For example, PCA of gene expression data will generate PCs that are linear combinations of thousands of genes and attempting to ascertain the biological relevance of such a large linear combination of genes is a very difficult task. The challenge of PC interpretation has motivated a large number of approaches for generating approximate PCs that have non-zero loadings for just a small subset of the measured variables. Such sparse PCA techniques include simple components (i.e., PC loading vectors constrained to values from $\{-1, 0, 1\}$) (Vines, 2000), methods which compute approximate PCs using cardinality constraints (d’Aspremont *et al.*, 2007; Moghaddam *et al.*, 2006; Sriperumbudur *et al.*, 2011; Tan *et al.*, 2018; Yuan and Zhang, 2013), methods that use LASSO or elastic net-based penalties (Jolliffe *et al.*, 2003; Jung *et al.*, 2019; Shen and Huang, 2008; Witten *et al.*, 2009; Zou *et al.*, 2006), and methods based on iterative component thresholding (Ma, 2013). By generating approximate PCs with few non-zero loadings, all of these techniques improve interpretability by associating only a small number of variables with each PC. For the comparative evaluation of our proposed approach, we will focus on three current sparse PCA techniques: SPC (Witten *et al.*, 2009), TPower (Yuan and Zhang, 2013) and rifle (Tan *et al.*, 2018). These methods represent both the cardinality constraint and LASSO-penalization approaches and have been shown to provide state-of-the-art performance in both simulation studies and real data analyses.

The Witten *et al.* SPC method has an elegant formulation via LASSO-penalized matrix decomposition. Specifically, SPC modifies the standard SVD matrix reconstruction optimization problem to include a LASSO penalty on the PC loadings. Using the notation introduced in Section 1.2, the SPC optimization problem for the first PC can be stated as:

$$\min_{d, \mathbf{u}, \mathbf{v}} \|\mathbf{X} - d\mathbf{u}\mathbf{v}^T\|_F^2 \text{ subject to } \|\mathbf{u}\|_2^2 = 1, \|\mathbf{v}\|_2^2 = 1, \sum_{i=1}^n |u_i| < c, d > 0 \quad (1)$$

Due to the LASSO penalty on the components of \mathbf{u} , this optimization problem generates a sparse version of the first PC loadings vector with the level of sparsity controlled by the parameter c .

Subsequent sparse PCs can be computed by iteratively applying SPC to the residual matrix generated by subtracting the rank 1 reconstruction $d\mathbf{u}\mathbf{v}^T$ from the original \mathbf{X} . Witten et al. also outline a more complex approach for computing multiple PCs that ensures orthogonality. Similar to LASSO-penalized generalized linear models (Tibshirani, 2011), the penalty parameter c can be specified to achieve a desired level of sparsity in the PC loadings or can be selected via cross-validation to minimize the average matrix reconstruction error. Since the true level of sparsity is typically not known, the cross-validation approach is usually employed to determine c and we will use this approach in our comparative evaluation. The need to estimate the sparsity parameter via a technique like cross-validation is not unique to SPC and is a limitation shared by all existing sparse PCA methods. A common alternative to picking c to minimize the average reconstruction error is to set c to the smallest value whose reconstruction error is within 1 standard error of the minimum error. This alternate version, which we will refer to as SPC.1se, generates a more sparse version of the PC loadings at the cost of increased reconstruction error.

Applying the SPC method as implemented in the PMA R package (Witten *et al.*, 2009) to compute sparse versions of the first two PCs of the example data simulated according to Section 1.3 generates the following sparse loadings when c is set to minimize the average cross-validation reconstruction error (note that orthogonality was not enforced and cross-validation was performed for just the first PC):

$$\hat{\mathbf{V}}_{\text{SPC}}, (\mathbf{1}, \mathbf{2})^T = \begin{bmatrix} -0.541 & -0.446 & -0.509 & -0.500 & 0 & 0 & 0 & 0 & -0.015 & -0.014 \\ 0.113 & -0.058 & -0.023 & -0.096 & 0.144 & -0.030 & 0 & -0.199 & 0.734 & 0.609 \end{bmatrix}$$

The SPC solution in this case generates zero loadings on the first PC for four of the six variables with a zero population loading. For the second PC, only one of the eight variables with a zero population loading is set to zero. As expected, the reconstruction error for this sparse solution is larger than that generated via PCA (598.148 vs. 597.531). If the SPC.1se variant is used instead, the following sparse loadings are produced:

$$\hat{\mathbf{V}}_{\text{SPC.1se}}, (\mathbf{1}, \mathbf{2})^T = \begin{bmatrix} -0.743 & -0.124 & -0.463 & -0.467 & 0 & 0 & 0 & 0 & 0 & 0 \\ 0.068 & -0.013 & -0.003 & -0.087 & 0.121 & 0 & 0 & -0.127 & 0.751 & 0.627 \end{bmatrix}$$

The SPC.1se solution does a better job of capturing the true sparsity of the PCs (all true zero loadings for the first PC are captured and two out of eight are captured for the second PC) at the cost of significantly increased reconstruction error (642.760 vs. 598.148).

The Yuan & Zhang TPower method solves the largest k -sparse eigenvalue problem, which has the following formulation for sparse PCA:

$$\max_{\mathbf{v}} \mathbf{v}^T \hat{\Sigma} \mathbf{v} \text{ subject to } \|\mathbf{v}\|_2 = 1, \|\mathbf{v}\|_0 \leq k \quad (2)$$

The TPower method solves this cardinality constrained optimization problem using a simple truncated version of the power iteration algorithm that truncates the estimated eigenvector on each iteration by setting all loadings to 0 except for the k loadings with the largest absolute values. Similar to the SPC method, the true PC cardinality k is usually unknown and must be estimated using cross-validation. Because an R version of the TPower method is not available, we have provided an implementation in the EESPCA R package along with cross-validation logic to select the sparsity parameter k . Using this TPower implementation, the first two sparse PC loading vectors for the running example are:

$$\hat{\mathbf{V}}_{\text{TPower}}, (\mathbf{1}, \mathbf{2})^T = \begin{bmatrix} 0.541 & 0.448 & 0.507 & 0.500 & 0 & 0 & 0 & 0 & 0 & 0 \\ 0 & 0 & 0 & 0 & 0 & 0 & 0 & 0 & 0.756 & 0.655 \end{bmatrix}$$

Similar to the SPC approach, the second sparse PC was generated by applying TPower to the residual matrix. In this case, the TPower method perfectly captures the true sparsity of the first two PCs. Given the sparser solution, the relative reconstruction error for TPower is larger than the error generated by SPC (604.896 vs. 598.148).

The Tan et al. rifle method solves the largest k -sparse generalized eigenvalue problem, which is identical to (2) in the context of PCA. For the rifle method, this optimization problem is solved using a two-stage approach that begins with a convex relaxation of (2) (Gao *et al.*, 2017) to generate an initial value of the principal eigenvector. This initialization step is followed by a non-convex optimization algorithm similar to the truncated power iteration of TPower that iteratively updates the generalized Rayleigh quotient followed by truncation of the estimated eigenvector to preserve the top k eigenvector loadings with the largest absolute values with all other loadings set to 0. Using the implementation in the rifle R package with cross-validation logic we implemented in the EESPCA package, the first two sparse PC loading vectors for the running example are:

$$\hat{\mathbf{V}}_{\text{rifle}}, (\mathbf{1}, \mathbf{2})^{\mathbf{T}} = \begin{bmatrix} 0.551 & 0.435 & 0.508 & 0.500 & 0 & 0 & 0 & 0 & 0 & 0 \\ 0 & 0 & 0 & 0 & 0 & 0 & 0 & 0 & 0.775 & 0.632 \end{bmatrix}$$

The second sparse PC was again generated by applying rifle to the residual matrix. Similar to TPower, the rifle method correctly estimates the true sparsity structure but with a slightly larger reconstruction error (605.066 vs. 604.896).

1.5 Eigenvectors from eigenvalues

Denton et al. (Denton *et al.*, 2020) recently published a survey of a fascinating association between the squared normed eigenvector elements of a Hermitian matrix and the eigenvalues of the full matrix and associated sub-matrices. This identity has a complex history in the mathematical literature with numerous rediscoveries in different disciplines since the earliest known reference in 1834 (Jacobi, 1834). Importantly in this context, the sample covariance matrix $\hat{\Sigma}$ is Hermitian, which implies that squared normed PC loadings can be computed as a function of PC variances for the full data set and all of the leave-one-out variable subsets. To briefly restate the results from Denton et al., let \mathbf{A} be a $p \times p$ Hermitian matrix with eigenvalues $\lambda_i(\mathbf{A})$ and normed eigenvectors \mathbf{v}_i for $i = 1, \dots, p$. Let the elements of each eigenvector \mathbf{v}_i be denoted $(\mathbf{v}_i)_j$ for $j = 1, \dots, p$. Let \mathbf{M}_j be the $(p-1) \times (p-1)$ submatrix of \mathbf{A} that results from removing the j^{th} column and the j^{th} row from \mathbf{A} . Denote the eigenvalues of \mathbf{M}_j by $\lambda_k(\mathbf{M}_j)$ for $k = 1, \dots, p-1$. Given these values, Denton et al. (Denton *et al.*, 2020) state their key result in Theorem 1:

Theorem 1 (from Denton *et al.* (2020)). *The norm squared of the elements of the eigenvectors are related to the eigenvalues and the submatrix eigenvalues:*

$$(|\mathbf{v}_i|_n)_j^2 = \prod_{k=1, k \neq i}^p (\lambda_i(\mathbf{A}) - \lambda_k(\mathbf{A})) = \prod_{k=1}^{p-1} (\lambda_i(\mathbf{A}) - \lambda_k(\mathbf{M}_j)) \quad (3)$$

Which can alternatively be represented as a ratio of the product of eigenvalue differences:

$$(|\mathbf{v}_i|_n)_j^2 = \frac{\prod_{k=1}^{p-1} (\lambda_i(\mathbf{A}) - \lambda_k(\mathbf{M}_j))}{\prod_{k=1, k \neq i}^p (\lambda_i(\mathbf{A}) - \lambda_k(\mathbf{A}))} \quad (4)$$

In the context of PCA, \mathbf{A} can be replaced by the sample covariance matrix $\hat{\Sigma}$ and (4) provides a formula for computing squared normed PC loadings from the PC variances of the full matrix and associated sub-matrices. It is important to note that this ratio is undefined (both numerator

and denominator are 0) under two degenerate scenarios: 1) when $(\mathbf{v}_i)_j = 0$, \mathbf{v}_i for \mathbf{A} will be an eigenvector for \mathbf{M}_j with the same eigenvalue, and 2) when \mathbf{A} has repeated eigenvalues. In the context of PCA on experimental data, however, these degenerate scenarios are extremely unlikely for the first k PCs as long as k is less than the rank of \mathbf{A} , so we can in practice safely assume that our approximation of (4) defined as (6) in Section 2.1 below is defined.

In the remainder of this paper, we will detail an approximation of (4) relevant to the sparse PCA problem, our proposed EESPCA method based on this approximation and results from a comparative evaluation of the EESPCA, SPC, SPC.1se, TPower and rifle techniques on simulated data and real data generated using single cell RNA-sequencing (Tanay and Regev, 2017; Wagner *et al.*, 2016). An R package implementing the EESPCA method and a vignette that contains the R logic used to generate the results for the simple running example can be found at <http://www.dartmouth.edu/~hrfrost/EESPCA>.

2 Methods

2.1 Approximate eigenvector from eigenvalue formulation

If \mathbf{A} is replaced by the sample covariance matrix $\hat{\Sigma}$, $\hat{\Sigma}_j$ represents the sample covariance sub-matrix with variable j removed, and computation focuses on the loadings for the first PC, (4) can be restated as:

$$(|\mathbf{v}_i|_n)_j^2 = \frac{\prod_{k=1}^{p-1} (\lambda_1(\hat{\Sigma}) - \lambda_k(\hat{\Sigma}_j))}{\prod_{k=2}^p (\lambda_1(\hat{\Sigma}) - \lambda_k(\hat{\Sigma}))} \quad (5)$$

Although a theoretically interesting result, (5) does not have obvious practical utility for PCA since it only generates squared normed values (i.e., it fails to capture the sign of the loading) and requires computation of the eigenvalues of all of the covariance sub-matrices. However, if we make the approximation that the eigenvalues $\lambda_i(\hat{\Sigma})$ for $i = 2, \dots, p-1$ are equal to the corresponding sub-matrix eigenvalues $\lambda_i(\hat{\Sigma}_j)$, many of the eigenvalue difference terms in (5) cancel and we can simplify as follows:

$$\begin{aligned} (|\mathbf{v}_1|_n)_j^2 &= \frac{\prod_{k=1}^{p-1} (\lambda_1(\hat{\Sigma}) - \lambda_k(\hat{\Sigma}_j))}{\prod_{k=2}^p (\lambda_1(\hat{\Sigma}) - \lambda_k(\hat{\Sigma}))} \\ (|\mathbf{v}_1|_n)_j^2 &= \frac{(\lambda_1(\hat{\Sigma}) - \lambda_1(\hat{\Sigma}_j))(\lambda_1(\hat{\Sigma}) - \lambda_2(\hat{\Sigma}_j)) \dots (\lambda_1(\hat{\Sigma}) - \lambda_{p-1}(\hat{\Sigma}_j))}{(\lambda_1(\hat{\Sigma}) - \lambda_2(\hat{\Sigma})) \dots (\lambda_1(\hat{\Sigma}) - \lambda_{p-1}(\hat{\Sigma})) (\lambda_1(\hat{\Sigma}) - \lambda_p(\hat{\Sigma}))} \\ (|\tilde{\mathbf{v}}_1|_n)_j^2 &= \frac{\lambda_1(\hat{\Sigma}) - \lambda_1(\hat{\Sigma}_j)}{\lambda_1(\hat{\Sigma}) - \lambda_p(\hat{\Sigma})} \end{aligned}$$

If we also assume that $\lambda_p(\hat{\Sigma}) \approx 0$, we can further simplify the approximate squared normed loadings $(|\tilde{\mathbf{v}}_1|_n)_j^2$ to:

$$(|\tilde{\mathbf{v}}_1|_n)_j^2 = 1 - \frac{\lambda_1(\hat{\Sigma}_j)}{\lambda_1(\hat{\Sigma})} \quad (6)$$

This approximation has several appealing properties in the context of sparse PCA. First, it greatly reduces the computational cost since only the largest eigenvalues of the full covariance matrix and associated sub-matrices are needed, which can be efficiently computed even for very large matrices using the method of power iteration. The computational cost can be further lowered by using the estimated principal eigenvector of the full matrix to initialize the power iteration calculation for the sub-matrices. When this approximation is applied to the population covariance matrix Σ , it

will correctly estimate zero squared loadings since $\lambda_1(\boldsymbol{\Sigma}) = \lambda_1(\boldsymbol{\Sigma}_j)$ for these variables; for variables that have a non-zero loading on the first population PC, the approximation will be less than or equal to the squared value of the true loading. For the example introduced in Section 1.3, the squared normed loadings for the first population PC are:

$$|\mathbf{v}_1|_n^2 = [0.25 \quad 0.25 \quad 0.25 \quad 0.25 \quad 0 \quad 0 \quad 0 \quad 0 \quad 0 \quad 0]$$

and the approximate squared normed loadings computed via (6) are:

$$|\tilde{\mathbf{v}}_1|_n^2 = [0.2 \quad 0.2 \quad 0.2 \quad 0.2 \quad 0 \quad 0 \quad 0 \quad 0 \quad 0 \quad 0]$$

When applied to the sample covariance matrix $\hat{\boldsymbol{\Sigma}}$, the approximate squared loadings will again be less than or equal to the squared PC loadings with the values for variables with a zero loading on the population PC approaching zero as $n \rightarrow \infty$ and $n/p \rightarrow \infty$ given the consistency of the sample PC loading vectors in this asymptotic regime (Johnstone and Lu, 2009). Importantly, the ratio of approximate-to-true loadings

$$(\mathbf{r})_j = \sqrt{(|\tilde{\mathbf{v}}_1|_n)_j^2 / (|\mathbf{v}_1|_n)_j^2} \tag{7}$$

will tend to be larger for variables that have a non-zero loading on the population PC than for variables with a zero population loading. This is due to the fact that the eigenvalue difference term retained in the numerator of the approximation, $\lambda_1(\hat{\boldsymbol{\Sigma}}) - \lambda_1(\hat{\boldsymbol{\Sigma}}_j)$, captures most of the squared loading value for variables with a true non-zero loading on the first population PC. If variable j only has a non-zero loading on the first population PC and $\lambda_p(\boldsymbol{\Sigma}) \approx 0$, then it follows from PCA consistency (Johnstone and Lu, 2009) that $(\mathbf{r}_1)_j \rightarrow 1$ as $n \rightarrow \infty$. On the other hand, variables that have a zero loading on the first population PC will have a sample loading that approaches 0 as $n \rightarrow \infty$ and, for finite n , have a non-zero value based on random contributions spread across the spectrum of eigenvalue difference terms. In this case, the approximation based on the difference term for just the largest eigenvalue, $\lambda_1(\hat{\boldsymbol{\Sigma}}) - \lambda_1(\hat{\boldsymbol{\Sigma}}_j)$, will tend to underestimate the sample loading by a greater degree than for variables with a true non-zero population PC loading. This property of approximation (6) provides important information regarding the true sparsity of the PC loadings and plays a key role in the EESPCA method detailed below. For the example data, the ratio (rounded to three decimal places) of approximate to real normed loadings for the first sample PC are:

$$\mathbf{r}_1 = [0.919 \quad 0.938 \quad 0.909 \quad 0.910 \quad 0.837 \quad 0.839 \quad 0.867 \quad 0.816 \quad 0.815 \quad 0.840]$$

Figure 1 illustrates the relationship between approximate and true squared loadings for first PC as computed on 1,000 data sets simulated according to the model in Section 1.3. As shown in this figure, the ratio for variables with a non-zero loading on the population PC is markedly larger on average than the ratio for variables with a zero population loading.

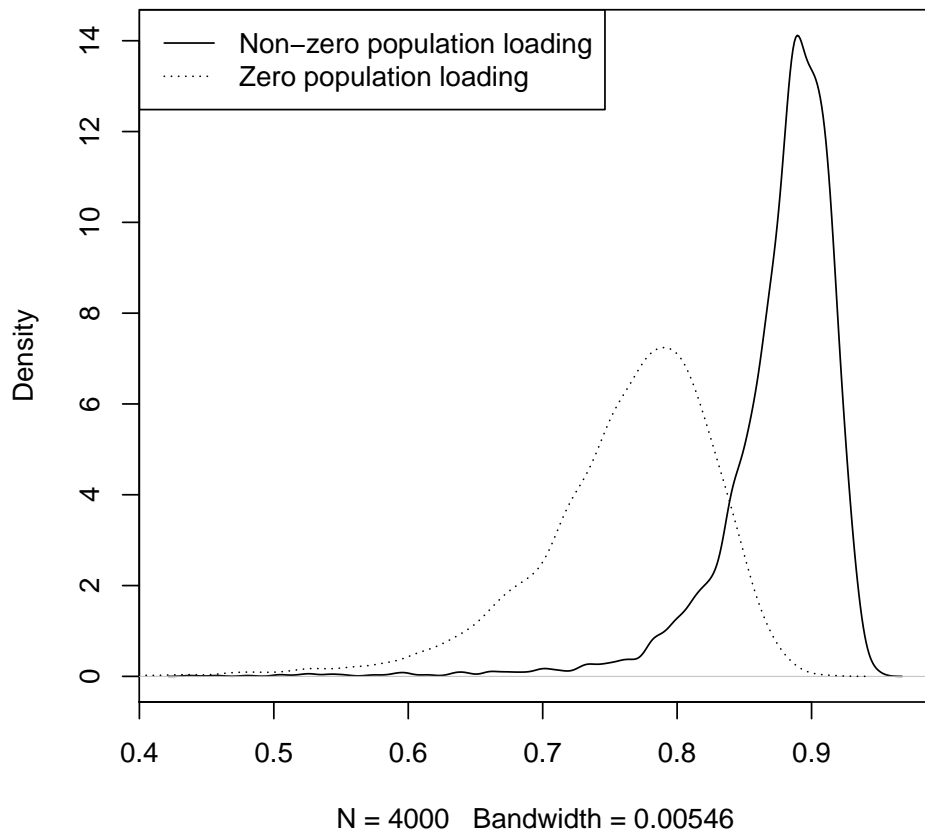


Figure 1: Kernel density estimates of the distribution of the ratio of approximate-to-real normed PC loadings. The ratio distribution for variables that have a non-zero loading on the population PC is shown as a solid line. The ratio distribution for variables that have a zero population loading is shown as a dashed line.

2.2 EESPCA

Algorithm 1 Eigenvectors from Eigenvalues Sparse PCA (EESPCA)

- Input:** $n \times p$ mean-centered matrix \mathbf{X}
Output: sparse first PC loadings vector \mathbf{v}_1^s and associated eigenvalue λ_1^s
- 1: $\hat{\Sigma} = 1/(n-1)\mathbf{X}^T\mathbf{X}$ ▷ Compute sample covariance matrix
 - 2: $\{\mathbf{v}_1, \lambda_1\} = \text{powerIteration}(\hat{\Sigma})$ ▷ Compute first eigenvector/eigenvalue
 - 3: $\forall_{j \in 1 \dots p} \lambda_1(\hat{\Sigma}_j) = \text{powerIteration}(\hat{\Sigma}_j)$ ▷ Compute first submatrix eigenvalues
 - 4: $\forall_{j \in 1 \dots p} (|\tilde{\mathbf{v}}_1|_n)_j^2 = 1 - \lambda_1(\hat{\Sigma}_j)/\lambda_1(\hat{\Sigma})$ ▷ Approximate first eigenvector using (6)
 - 5: $\forall_{j \in 1 \dots p} (\mathbf{r}_1)_j = \sqrt{(|\tilde{\mathbf{v}}_1|_n)_j^2 / (|\mathbf{v}_1|_n)_j^2}$ ▷ Compute ratio of norm squared eigenvectors
 - 6: Compute sparse \mathbf{v}_1^s using \mathbf{r}_1 :
 - a: $\mathbf{v}_1^s = \mathbf{r}_1 \odot \mathbf{v}_1$ ▷ Scale \mathbf{v}_1 by \mathbf{r}_1
 - b: $\mathbf{v}_1^s = |\mathbf{v}_1^s|_n$ ▷ Normalize \mathbf{v}_1^s to unit length
 - c: Set $(\mathbf{v}_1^s)_j = 0$ for all $(\mathbf{v}_1^s)_j < 1/\sqrt{p}$ ▷ Truncate \mathbf{v}_1^s using threshold $1/\sqrt{p}$
 - d: $\mathbf{v}_1^s = |\mathbf{v}_1^s|_n$ ▷ Normalize \mathbf{v}_1^s to unit length
 - 7: $\lambda_1^s = (\mathbf{v}_1^s)^T \hat{\Sigma} \mathbf{v}_1^s$ ▷ Compute sparse first eigenvalue
-

Our proposed EESPCA method, which is based on the eigenvector from eigenvalue approximation (6) detailed above, computes a sparse version of the first sample PC for mean-centered $n \times p$ matrix \mathbf{X} using Algorithm 1 with additional details for each step as follows:

1. Compute the unbiased sample covariance matrix $\hat{\Sigma} = 1/(n-1)\mathbf{X}^T\mathbf{X}$.
2. Use the power iteration method to compute the principal eigenvector \mathbf{v}_1 and associated eigenvalue λ_1 of $\hat{\Sigma}$.
3. Use the power iteration method to compute the principal eigenvalues of the sub-matrices, $\lambda_1(\hat{\Sigma}_j)$. For efficient calculation, the power iteration method is used with the initial value set to a subsetted version of \mathbf{v}_1 , i.e., \mathbf{v}_1 with the relevant variable removed.
4. Use formula (6) to approximate the squared normed principal eigenvector $|\tilde{\mathbf{v}}_1|_n^2$.
5. Compute the element-wise ratio of approximate-to-real normed eigenvectors: $(\mathbf{r}_1)_j = \sqrt{(|\tilde{\mathbf{v}}_1|_n)_j^2 / (|\mathbf{v}_1|_n)_j^2}$.
6. Use \mathbf{r}_1 to compute a sparse version of \mathbf{v}_1 . As outlined in Section 2.1 above, the entries in \mathbf{r}_1 will be less than one and will tend to be larger for variables with a non-zero population loading than for variables with a zero population loading. This property suggests that one could use \mathbf{r}_1 to scale \mathbf{v}_1 followed by renormalization to generate sample PC loadings that more closely match the population loadings, however, this would not generate sparse loadings since the elements of \mathbf{r}_1 are themselves non-zero. To produce a sparse version of \mathbf{v}_1 , we follow the initial scaling and renormalization with a thresholding operation that sets any adjusted loadings less than $1/\sqrt{p}$ (element of a unit length vector that has identical values) to 0 and then renormalize a final time to produce a sparse and unit length loadings vector \mathbf{v}_1^s . Specifically:
 - (a) Scale \mathbf{v}_1 by \mathbf{r}_1 , i.e., set \mathbf{v}_1^s to the element-wise product of \mathbf{v}_1 and \mathbf{r}_1 .
 - (b) Normalize \mathbf{v}_1^s , i.e., $\mathbf{v}_1^s = |\mathbf{v}_1^s|_n = \mathbf{v}_1^s / \|\mathbf{v}_1^s\|_2$.
 - (c) Truncate \mathbf{v}_1^s by setting $(\mathbf{v}_1^s)_j = 0$ for all $(\mathbf{v}_1^s)_j < 1/\sqrt{p}$

(d) Normalize \mathbf{v}_1^s again to generate a sparse and unit length eigenvector.

7. Compute the associated eigenvalue λ_1^s as:

$$\lambda_1^s = (\mathbf{v}_1^s)^T \hat{\Sigma} \mathbf{v}_1^s \quad (8)$$

To compute multiple sparse PCs, the EESPCA method uses a similar approach to that employed by the SPC method, i.e., it repeatedly applies to the procedure outlined above for calculating the first sparse PC to the residual matrix formed by subtracting the rank 1 reconstruction of \mathbf{X} generated using \mathbf{v}_1^s from the input \mathbf{X} . Note that multiple sparse PCs generated using this recursive approach are not guaranteed to be orthogonal. When applied to the example data described in Section 1.3, the EESPCA method produces the following sparse PC loading vectors (rounded to three decimal places):

$$\hat{\mathbf{V}}_{\text{EESPCA}}, (\mathbf{1}, \mathbf{2})^T = \begin{bmatrix} 0.543 & 0.457 & 0.503 & 0.494 & 0 & 0 & 0 & 0 & 0 & 0 \\ 0 & 0 & 0 & 0 & 0 & 0 & 0 & 0.779 & 0.627 & 0 \end{bmatrix}$$

Similar to the TPower and rifle methods, the EESPCA method correctly estimates the true population sparsity structure. This is in contrast to SPC, which had nine errors, and SPC.1se, which had six errors. The reconstruction error for the EESPCA solution (605.072) was very close to the error for the TPower (604.896) and rifle (605.067) methods. Although EESPCA, TPower and rifle all work very well on this simple example, the relative performance diverges in other regions of the data model space as explored in Section 3.1

2.3 Simulation study design

To explore the comparative performance of the EESPCA, SPC, SPC.1se, TPower and rifle methods, we simulated MVN data for a range of sample sizes, variable dimensionality and covariance structures. Although *.1se variants of TPower and rifle are also possible, we are only showing results for SPC.1se since the relative performance pattern is similar. Specifically, we simulated data sets containing n independent samples drawn from a p -dimensional MVN data with a zero population mean vector and population covariance matrix Σ with all variances set to 1 and all covariances set to 0 except for the covariances between the first $b \geq 2$ variables, which were set to a non-zero ρ . According to this Σ , the first population PC will have equal, non-zero loadings for the first b variables and zero loadings for the remaining $p - b$ variables. Data was simulated for a range of n , p , b and ρ values with 50 data sets generated per unique parameter combination.

The EESPCA, SPC, SPC.1se, TPower and rifle methods were used to compute the first sparse PC of each simulated data set and method performance was quantified according to classification accuracy (i.e., ability of method to correctly assign zero loadings to variables that with a zero population loading), computational speed and reconstruction error. Specifically, the specificity, sensitivity and balanced accuracy of each method were computed. If v_i and v_i^s represent the i^{th} elements of the true eigenvector \mathbf{v} and sparse estimate \mathbf{v}^s and $1(\cdot)$ is the indicator function, then the sensitivity is defined as $\text{sens} = \sum_{i=1}^p 1(v_i^s = 0 \wedge v_i = 0) / \sum_{i=1}^p 1(v_i = 0)$ (i.e., the proportion of true zero loadings recovered by the sparse PCA method), specificity is defined as $\text{spec} = \sum_{i=1}^p 1(v_i^s \neq 0 \wedge v_i \neq 0) / \sum_{i=1}^p 1(v_i \neq 0)$ (i.e., the proportion of true non-zero loadings recovered by the sparse PCA method), and balanced accuracy is defined as $\text{balacc} = (\text{sens} + \text{spec}) / 2$. The SPC and SPC.1se methods were realized using the $\text{SPC}()$ method in version 1.2.1 of the PMA R package (Witten *et al.*, 2009) with the optimal penalty parameter computed using the $\text{SPC.cv}()$ method with $\text{nfolds}=5$, $\text{niter}=10$ and $\text{sumabsv}=\text{seq}(1, \text{sqrt}(p), \text{len}=20)$. We created

an R implementation of the TPower algorithm, which is available in the EESPCA R package via the function *tpower()*. The initial eigenvector for the TPower algorithm was computed using non-truncated power iteration. To determine the optimal cardinality parameter k for TPower, we implemented a cross-validation method based on the *SPC.cv()* function. This cross-validation method is available in the EESPCA R package via the function *tpowerPCACV()* and was executed for the simulation studies using $nfolds=5$ and $k.value=round(seq(1, p, len=20))$. The rifle method was realized using the *rifle()* function in version 1.0 of the rifle R package. The initial eigenvector for the rifle method was computed using the suggested *initial.convex()* function from the rifle R package using $K = 1$ and $lambda = sqrt(log(p)/n)$ (this is implemented in the EESPCA R package using the convenience function *rifleInit()*). Similar to the TPower method, the optimal cardinality parameter k for rifle was computed using the Witten et al. cross-validation approach as implemented by the *riflePCACV()* function in the EESPCA R package with $nfolds=5$ and $k.value=round(seq(1, p, len=20))$.

2.4 Real data analysis design

To explore the performance of the EESPCA, SPC, SPC.1se, TPower and rifle methods on real data, we analyzed a single cell RNA-sequencing (scRNA-seq) data set generated on 2.7k human peripheral blood mononuclear (PBMC) cells. This scRNA-seq data set is freely available from 10x Genomics and is used in the Guided Clustering Tutorial (Seurat, 2020) for the Seurat single cell framework (Stuart *et al.*, 2019). Preprocessing, quality control (QC) and normalization of the PBMC data set followed the same processing steps used in the Seurat Guided Clustering Tutorial. Specifically, the Seurat log-normalization method was used followed by application of the *vst* method for decomposing technical and biological variance. Seurat log-normalization divides the unique molecular identifier (UMI) counts for each gene in a specific cell by the sum of the UMI counts for all genes measured in the cell and multiplies this ratio by the scale factor 1×10^6 . The normalized scRNA-seq values are then generated by taking the natural log of this relative value plus 1. This technique generates normalized data whose non-zero values can be approximated by a log-normal distribution. The Seurat *vst* method fits a non-linear trend to the log scale variance/mean relationship. This estimated trend models the expected technical variance based on mean gene expression; observed variance values above this expected trend reflect biological variance. Preprocessing and QC of the PBMC data yielded normalized counts for 14,497 genes and 2,638 cells. Immune cell types were assigned using the same procedure detailed in the Seurat Guided Clustering Tutorial.

The 1,000 genes with the largest estimated biological variance according to the *vst* method were used as input for standard PCA, EESPCA, SPC, SPC.1se, TPower and rifle. Only the first two sparse PCs were generated using the five sparse PCA methods, which were executed using the same parameter settings as detailed in Section 2.3. Gene Ontology (GO) (Gene Ontology Consortium, 2010) enrichment analysis was used to interpret the normal and sparse PCs. Specifically, the *goana()* method (Young *et al.*, 2010) in the *limma* R package (Ritchie *et al.*, 2015) was used to determine the statistical enrichment of GO Biological Process Ontology terms among genes with either positive or negative PC loadings. The *goana()* method performs this enrichment analysis using a Fisher’s exact test on the 2×2 contingency table that categorizes the 1,000 high variance genes according to whether they belong to the target GO term and whether they have a positive (or negative) loading on the target PC. False discovery rate (FDR) values were computed using the Benjamini and Hochberg method (Benjamini and Hochberg, 1995) separately for each PC and loading direction for the family of test corresponding to all GO Biological Process terms.

3 Results and discussion

3.1 Classification performance

As illustrated in Figure 2, the EESPCA method has superior classification performance (as measured by balanced accuracy) relative to the other methods across the full range of simulation models with the difference particularly pronounced at low parameter values. As expected, the accuracy of all methods tends to increase as either n , ρ or b increase; improved performance at larger p with n fixed was unexpected. In contrast to EESPCA and SPC.1se, the accuracy of the SPC method plateaus and then declines at high parameter values. The TPower and rifle methods have similar performance which converges with EESPCA at higher parameter values (TPower is slightly more accurate than rifle at smaller parameter values). The corresponding sensitivity (i.e., ability to assign zero loadings for variables with a zero population loading) and specificity (i.e., ability to assign a non-zero loading to variables with a non-zero population loading) values, shown in Figures 3 and 4, provide more insight into the relative performance of the methods. Looking at the sensitivity plots in Figure 3, the SPC.1se method had almost perfect sensitivity, which is consistent with the fact that the SPC.1se method generates a much sparser solution than the SPC variant. The sensitivity plots also demonstrate that the poor balanced accuracy of the SPC method on higher parameter values is due largely to poor specificity, i.e, the SPC solution, which is driven by the minimization of reconstruction error, is insufficiently sparse at these parameter values. The specificity plots in Figure 4 match the general trend in balanced accuracy, with the specificity for EESPCA and SPC quickly approaching 1 as parameter values are increased. In contrast, the SPC.1se method has much lower specificity, which is expected given the sparser solution generated by this approach. Overall, EESPCA is able to achieve high sensitivity and specificity for almost all simulation models.

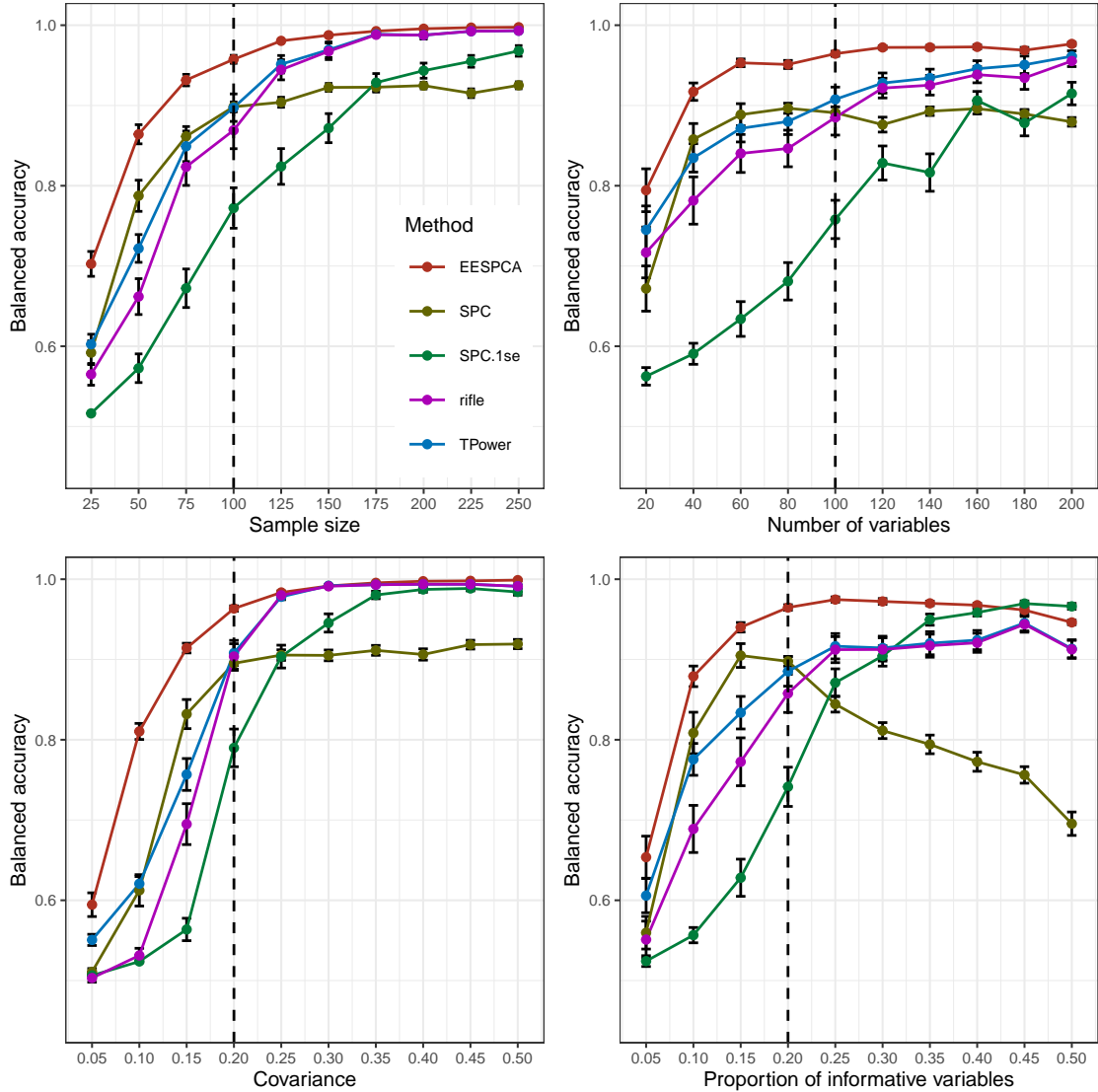


Figure 2: Classification performance of EESPCA, SPC, SPC.1se, TPower and rifle on data simulated using the procedure detailed in Section 2.3. Each panel illustrates the relationship between the balanced accuracy of the methods (i.e., the ability to correctly assign 0 loadings to variables with a 0 population loading) and one of the simulation parameters. The vertical dotted lines mark the default parameter value used in the other panels. Error bars represent ± 1 SE.

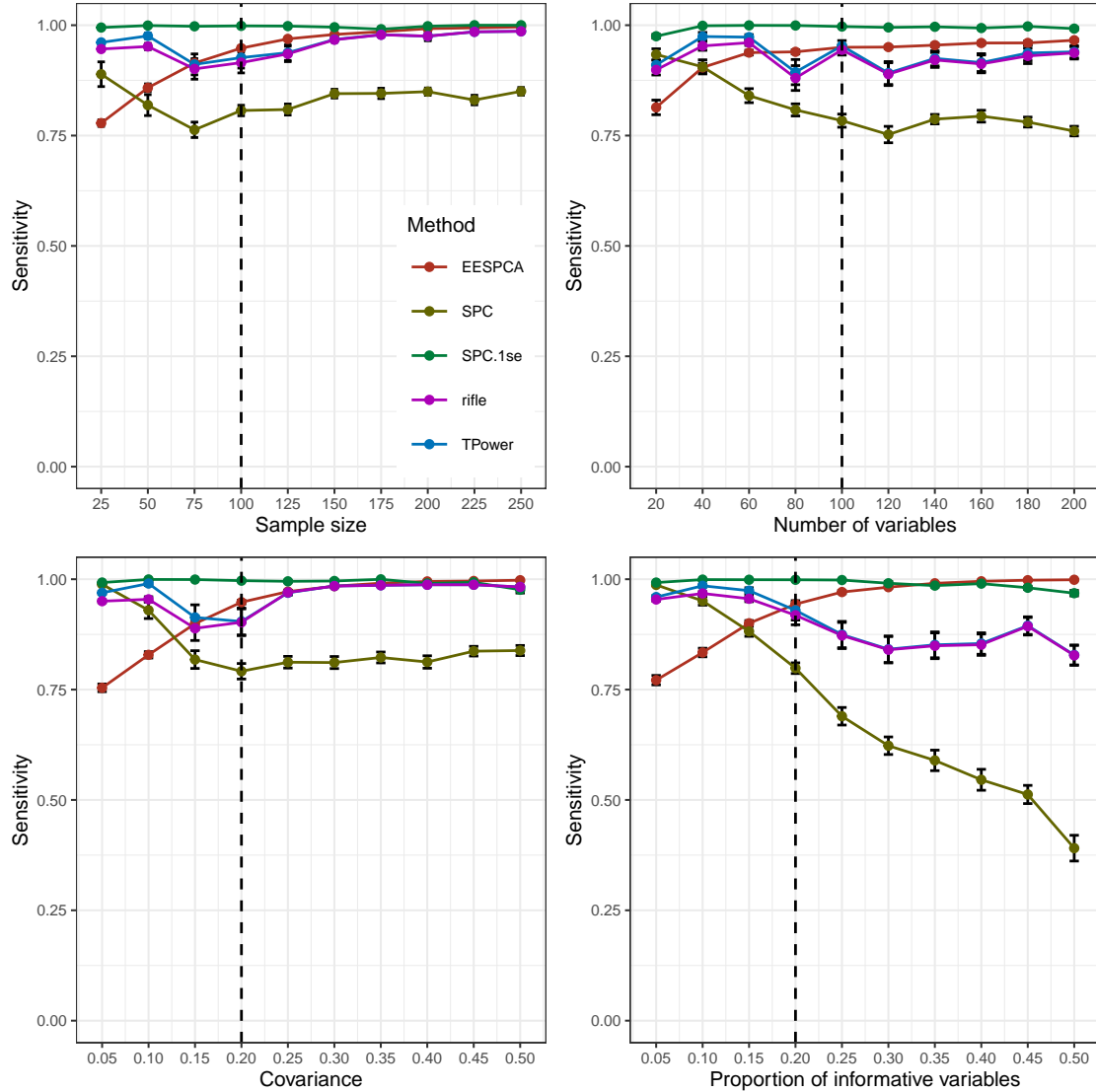


Figure 3: Sensitivity of EESPCA, SPC, SPC.1se, TPower and rifle on data simulated using the procedure detailed in Section 2.3. Each panel illustrates the relationship between sensitivity (i.e., the proportion of variables with a zero population loading that are given a zero loading in the estimated sparse PC) and one of the simulation parameters. The vertical dotted lines mark the default parameter value used in the other panels. Error bars represent ± 1 SE.

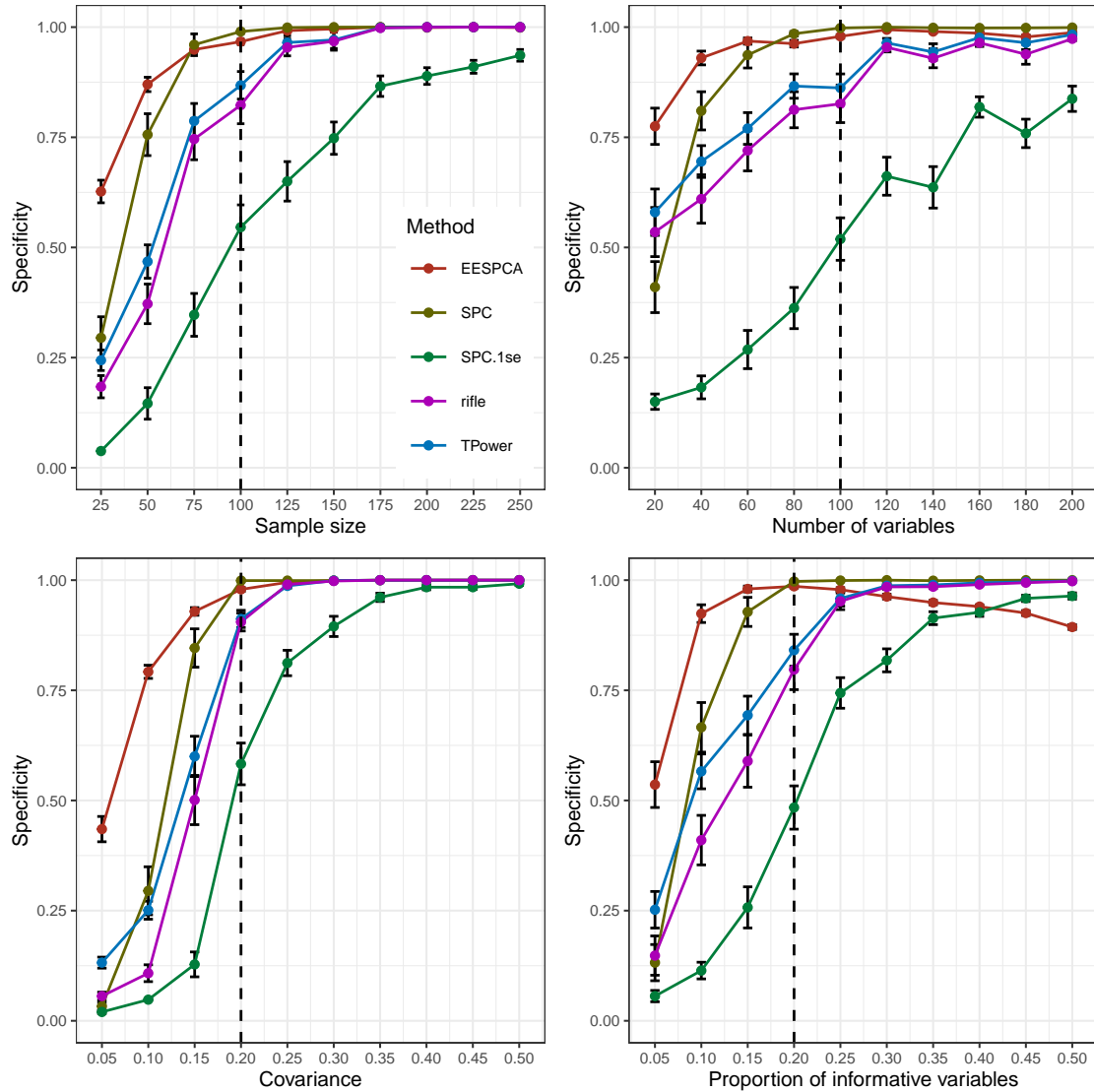


Figure 4: Specificity of EESPCA, SPC, SPC.1se, TPower and rifle on data simulated using the procedure detailed in Section 2.3. Each panel illustrates the relationship between specificity (i.e., the proportion of variables with a non-zero population loading that are given a non-zero loading in the estimated sparse PC) and one of the simulation parameters. The vertical dotted lines mark the default parameter value used in the other panels. Error bars represent ± 1 SE.

3.2 Computational speed

Figure 5 illustrates the relative computational cost of the evaluated methods. Because the SPC.1se and SPC methods have equivalent computational cost, the lines overlap and only the SPC.1se values are visible. As shown in this figure, the execution time of the SPC and TPower methods is close to two-orders-of-magnitude larger than the execution time for the EESPCA method for almost all parameter settings. The rifle method by contrast is nearly three-orders-of-magnitude slower than EESPCA. These dramatic differences in computational cost are primarily driven by the required cross-validation-based selection of sparsity constraints for SPC, SPC.1se, TPower and rifle. As expected, computational speed is fairly insensitive to changes in ρ or b for all methods and tends to increase as either n or p are increased (though execution time for both EESPCA and rifle is insensitive to sample size across the range of tested n values).

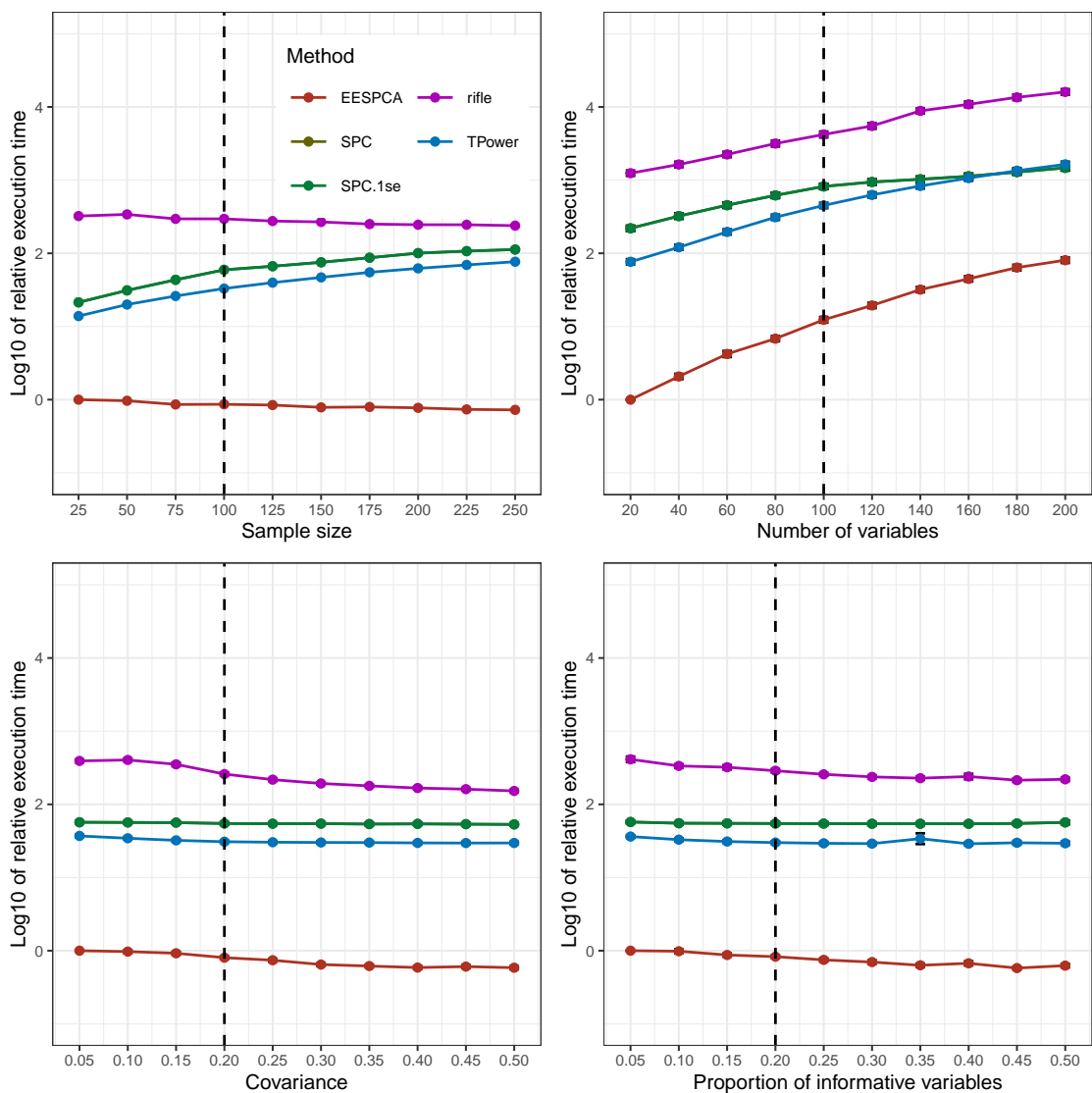


Figure 5: Relative computational speed of EESPCA, SPC, SPC.1se, TPower and rifle on data simulated using the procedure detailed in Section 2.3. Each panel illustrates the relationship between the relative computational speed of each method (i.e., \log_{10} ratio of computational cost of the method and the cost of the EESPCA method on data simulated using the smallest parameter value shown on the x-axis) and one of the simulation parameters. The SPC and SPC.1se lines overlap given the identical computational times. The vertical dotted lines mark the default parameter value used in the other panels. Error bars represent ± 1 SE.

3.3 Reconstruction error

Figure 6 shows the relative rank 1 reconstruction error for the evaluated sparse methods as compared to the reconstruction error for standard PCA. As expected, the error for all methods decreases as parameter values increase with SPC.1se producing the largest error for all models. Although the SPC method has the lowest error for most simulation models, the EESPCA error is lower at small parameter values and only slightly higher for larger settings.

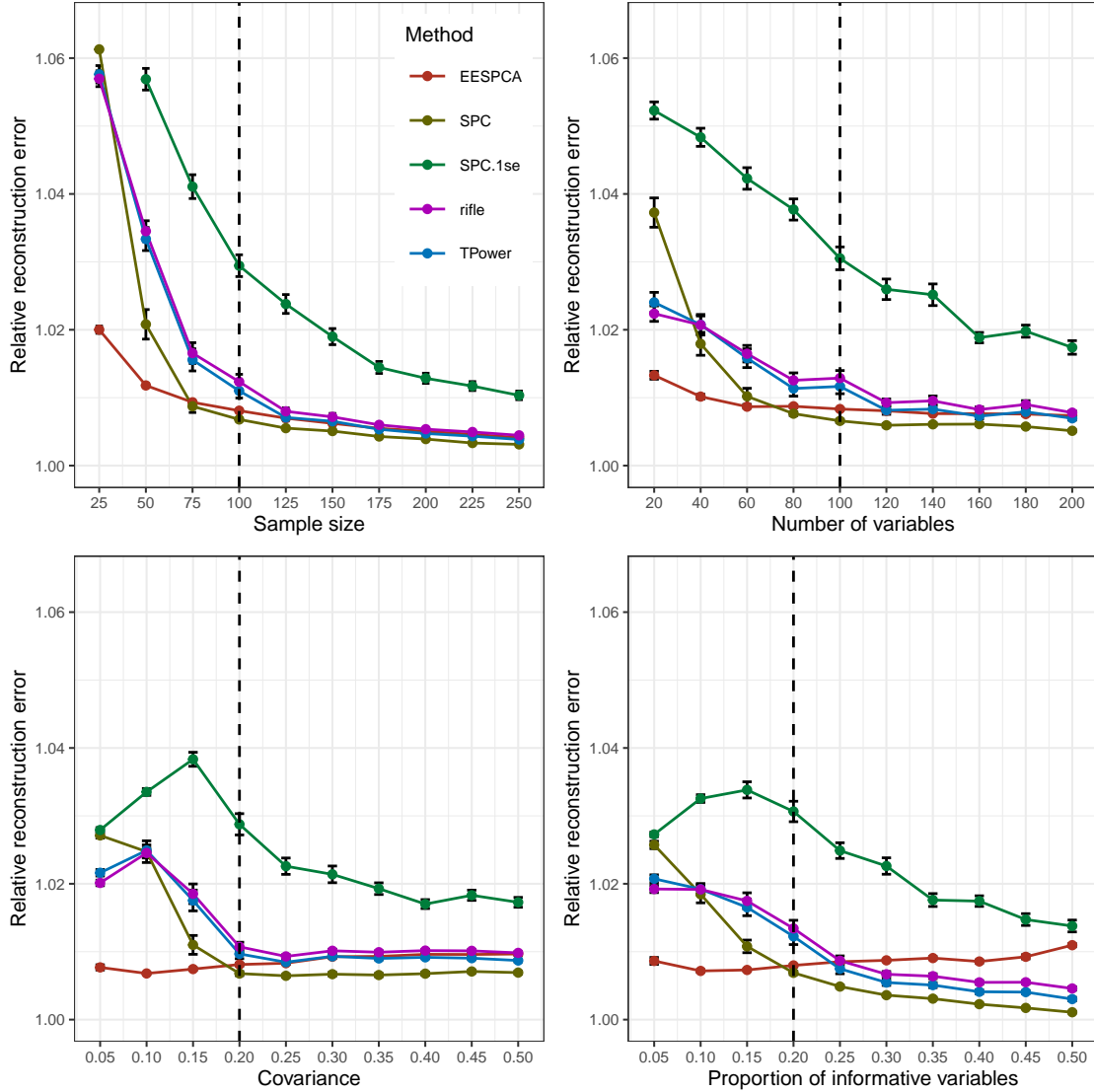


Figure 6: Rank 1 reconstruction error of EESPCA, SPC, SPC.1se, TPower and rifle on data simulated using the procedure detailed in Section 2.3. Each panel illustrates the relationship between the ratio of the rank 1 reconstruction error (i.e., squared Frobenius norm of the residual matrix formed by subtracting the rank 1 reconstruction matrix from the original matrix) for each method to the optimal error achieved by standard PCA. The vertical dotted lines mark the default parameter value used in the other panels. Error bars represent ± 1 SE.

3.4 Real data analysis

As detailed in Section 2.4, standard PCA, EESPCA, SPC, SPC.1se, TPower and rifle were applied to a scRNA-seq data set that captured the expression values of the 1,000 genes with the largest estimated biological variance for 2,638 individual human immune cells. Figure 7 illustrates the projection of these cells onto the first two standard or sparse PCs computed using these methods. Similar to the simulation results, the EESPCA method was close to 2 orders-of-magnitude faster than SPC or SPC.1se (20.87 seconds vs. 25.92 minutes on a standard laptop). The TPower method was markedly slower, taking 57.12 minutes. Because the rifle method is more than an order of magnitude slower than SPC, cross-validation was not performed for this data set and the optimal k values computed for TPower were used instead; even without cross-validation, execution of rifle still took 7.08 minutes. Qualitatively, all of the methods generate a very similar projection with the first PC separating cytotoxic from non-cytotoxic cells and the second PC capturing phenotypic differences among the non-cytotoxic populations.

Table 1 lists various statistics for first two normal or sparse PCs computed by each of these methods on the PBMC scRNA-seq data. Standard PCA assigned a non-zero loading to all genes on both PCs and GO enrichment analysis based on these loadings only produced significant findings for genes associated with PC 1 (49 significant terms for genes with a positive sign and 1 for genes with a negative sign). The SPC method generated very little sparsity on this data set with GO enrichment results similar to those generated by standard PCA. As expected, the SPC.1se method produced sparser PCs than the SPC method, which increased the number of significant GO terms for PC 1 and allowed 16 GO terms to reach significance for the positive direction on PC 2. TPower produced no zero loadings for the first PC so had enrichment results identical to standard PCA. For PC 2, TPower generated some sparsity with 3 significant GO terms for the positive direction. Because rifle was executed with the same cardinality constraints as TPower, it also produced no sparsity for PC 1 and only moderate sparsity for PC 2 with similar numbers of significant GO terms. The EESPC method generated the most sparse solution on this scRNA-seq data, which enabled GO enrichment analysis to produce significant results for three of the four test cases. All of the sparse PCA methods had reconstruction errors less than one percent larger than the optimal error from PCA with the SPC error very similar to the PCA error. Table 2 below lists the five most significant GO terms for each test case and method. Importantly, these results mirror the expected interpretation of the first two PCs. These results also highlight a well known challenge with hierarchical gene set collections like the Gene Ontology, namely that the ranked result list will contain sequences of biologically similar and highly overlapping gene sets.

	PC 1				PC 2				Relative reconstruction error
	Positive		Negative		Positive		Negative		
	genes	sig. GO	genes	sig. GO	genes	sig. GO	genes	sig. GO	
PCA	558	49	442	1	316	0	684	0	1
EESPCA	134	104	12	0	35	39	83	3	1.006
SPC	535	41	418	0	316	0	684	0	1.00001
SPC.1se	267	88	100	0	120	16	394	0	1.003
TPower	558	49	442	1	203	3	587	0	1.00001
rifle	558	49	442	1	249	3	541	0	1.0005

Table 1: Results from standard PCA, EESPC, SPC, SPC.1se, TPower and rifle analysis of the PBMC scRNA-seq data following the procedure detailed in Section 2.4. The table lists the number of the 1,000 genes in the input data matrix that were assigned positive or negative loadings. Since standard PCA produces non-zero loadings for all genes, the magnitude of the difference between the PCA counts and the counts for the other methods reflects the relative sparsity of the solutions. The "sig. GO" columns capture the number of Gene Ontology Biological Process terms that were significantly enriched among the genes with either positive or negative loadings at an FDR of ≤ 0.1 . The relative reconstruction error captures the squared Frobenius norm of the residual matrix for the first two PCs relative to the error from standard PCA.

	Gene Ontology term	# genes in term	# genes in group	FDR
PCA (PC 1, pos)	secretion	139	113	1.74e-07
	export from cell	135	110	2.60e-07
	secretion by cell	132	107	9.85e-07
	vesicle-mediated transport	172	133	1.92e-06
	exocytosis	101	84	1.22e-05
PCA (PC 1, neg)	ncRNA metabolic process	41	32	0.035
EESPCA (PC 1, pos)	immune response	200	69	8.12e-15
	immune system process	253	76	5.76e-13
	immune effector process	129	49	1.48e-10
	defense response	140	51	2.64e-11
	neutrophil activation	69	34	5.06e-10
EESPCA (PC 2, pos)	adaptive immune response	51	17	1.72e-10
	antigen receptor-mediated signaling pathway	35	12	2.14e-06
	antigen processing and presentation of exogenous peptide antigen via MHC...	16	9	2.36e-06
	antigen processing and presentation of peptide antigen via MHC class II	17	9	4.88e-06
	antigen processing and presentation of peptide or polysaccharide antigen...	17	9	2.32e-06
EESPCA (PC 2, neg)	regulation of transport	103	23	0.0057
	regulation of localization	154	28	0.024
	positive regulation of transport	59	16	0.027
SPC (PC 1, pos)	secretion	139	111	6.38e-08
	export from cell	135	108	1.07e-07
	vesicle-mediated transport	172	131	3.21e-07
	secretion by cell	132	105	4.40e-07
	exocytosis	101	84	6.75e-07
SPC.1se (PC 1, pos)	immune system process	253	121	2.65e-13
	immune effector process	129	75	4.99e-12
	immune response	200	101	4.99e-12
	vesicle-mediated transport	172	89	9.46e-11
	leukocyte mediated immunity	94	59	1.10e-10
SPC.1se (PC 2, pos)	adaptive immune response	51	27	2.11e-09
	B cell receptor signaling pathway	8	8	2.91e-04
	antigen receptor-mediated signaling pathway	35	17	5.14e-04
	B cell activation	22	13	1.02e-03
	immune response	200	47	2.17e-03
TPower (PC 1, pos)	<i>Same as PCA</i>			
TPower (PC 1, neg)	<i>Same as PCA</i>			
TPower (PC 2, pos)	adaptive immune response	51	27	0.00070
	B cell receptor signaling pathway	8	8	0.018
	B cell activation	22	14	0.064
rifle (PC 1, pos)	<i>Same as PCA</i>			
rifle (PC 1, neg)	<i>Same as PCA</i>			
rifle (PC 2, pos)	adaptive immune response	51	30	0.00076
	B cell activation	22	16	0.016
	B cell receptor signaling pathway	8	8	0.093

Table 2: Gene Ontology (GO) enrichment results for positive and negatives loadings on first two PCs generated by standard PCA, EESPC, SPC, SPC.1se, TPower and rifle analysis of the PBMC scRNA-seq data. The top five GO Biological Process terms with an FDR of ≤ 0.1 are listed.

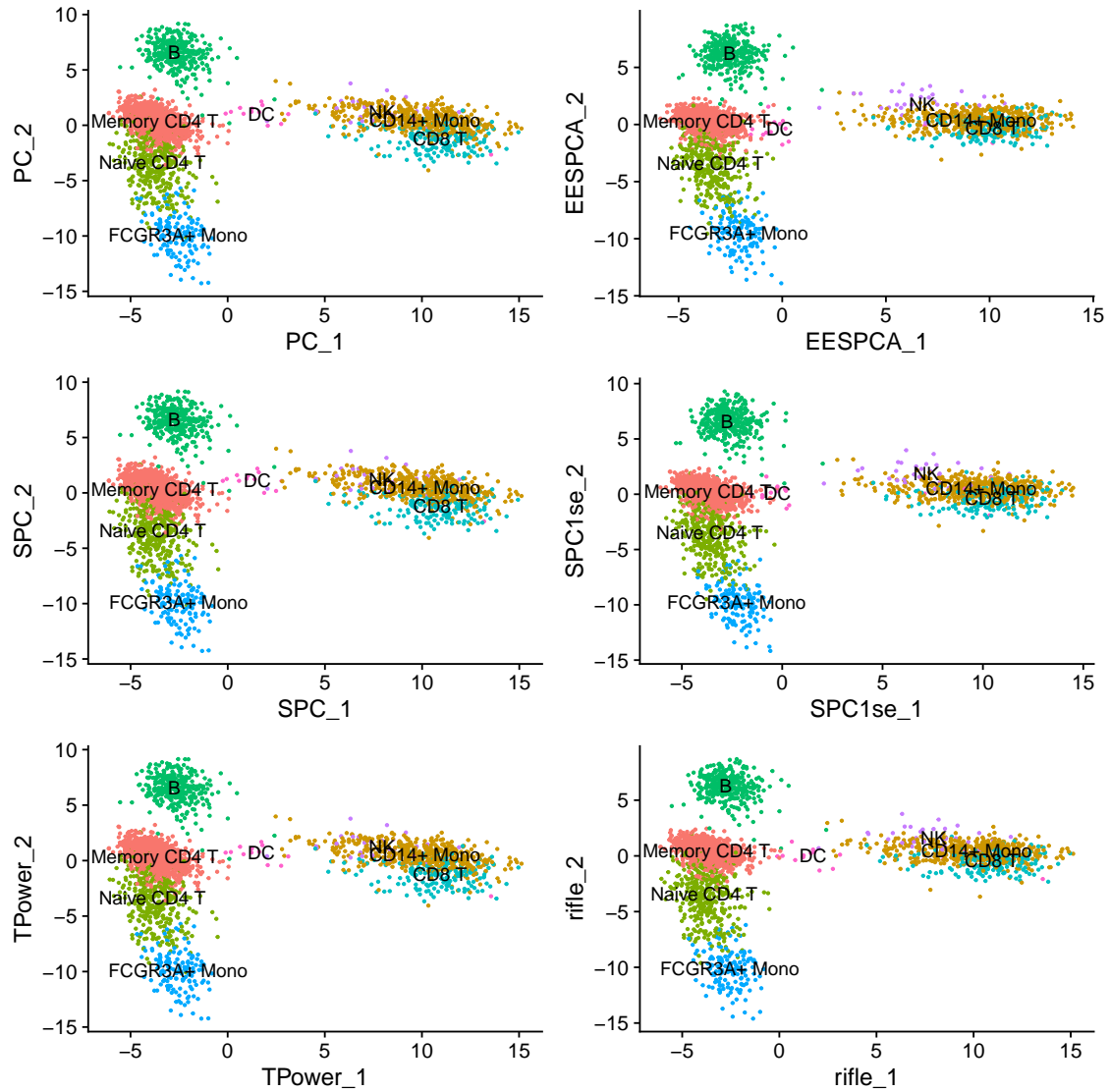


Figure 7: Projections of the PBMC 2k single cell RNA-sequencing data onto the first two PC computed using standard PCA or the first two sparse PCs computed using the EESPCA, SPC, SPC.1se, TPower or rifle method. Each point represents a single cell is colored and labeled according to immune cell type as detailed in the Seurat Guided Clustering Tutorial Seurat (2020).

4 Conclusions

The EESPCA method is a novel sparse PCA technique based on an approximation of the recently rediscovered formula for calculating eigenvectors from eigenvalues for Hermitian matrices (Denton *et al.*, 2020). Compared to the state-of-the-art SPC (and SPC.1se variant) (Witten *et al.*, 2009), TPower (Yuan and Zhang, 2013) and rifle (Tan *et al.*, 2018), EESPCA can more accurately estimate the true population sparsity structure at a dramatically lower computational cost without the need for stochastic sparsity parameter tuning via cross-validation. Importantly, EESPCA provides improved classification accuracy and lower computational cost without significantly increasing the reduced rank matrix reconstruction error. For analysis problems that prioritize correct estimation of the PC sparsity structure, EESPCA should be preferred over SPC, SPC.1se, TPower and rifle. EESPCA should also be preferred for computationally demanding problems, such as the analysis of very large data matrices generated by techniques like scRNA-seq or the use of statistical methods like resampling that require repeated application of sparse PCA. If minimization of reconstruction error is the key goal, a less sparse solution is acceptable and computational speed is not a major concern, then the SPC method is preferable to EESPCA unless $p > n$, the true sparsity of the PC is large (i.e., $> 90\%$) or the covariance between variables with a true non-zero loading is small.

Acknowledgments

This work was funded by National Institutes of Health grants K01LM012426, R21CA253408, P20GM130454 and P30CA023108. We would like to acknowledge the supportive environment at the Geisel School of Medicine at Dartmouth where this research was performed.

References

- Benjamini, Y. and Hochberg, Y. (1995). Controlling the false discovery rate: a practical and powerful approach to multiple testing. *Journal of the Royal Statistical Society. Series B (Statistical Methodology)*, pages 289–300.
- d’Aspremont, A., El Ghaoui, L., Jordan, M. I., and Lanckriet, G. R. G. (2007). A direct formulation for sparse PCA using semidefinite programming. *SIAM Review*, **49**(3), 434–448.
- Denton, P. B., Parke, S. J., Tao, T., and Zhang, X. (2020). Eigenvectors from eigenvalues: a survey of a basic identity in linear algebra. arXiv:1908.03795v3.
- Fan, J., Salathia, N., Liu, R., Kaeser, G. E., Yung, Y. C., Herman, J. L., Kaper, F., Fan, J.-B., Zhang, K., Chun, J., and Kharchenko, P. V. (2016). Characterizing transcriptional heterogeneity through pathway and gene set overdispersion analysis. *Nat Methods*, **13**(3), 241–4.
- Gao, C., Ma, Z., and Zhou, H. H. (2017). Sparse cca: Adaptive estimation and computational barriers. *Ann. Statist.*, **45**(5), 2074–2101.
- Gene Ontology Consortium (2010). The gene ontology in 2010: extensions and refinements. *Nucleic Acids Res*, **38**(Database issue), D331–5.
- Hafemeister, C. and Satija, R. (2019). Normalization and variance stabilization of single-cell rna-seq data using regularized negative binomial regression. *Genome Biol*, **20**(1), 296.

- Hastie, T., Tibshirani, R., and Friedman, J. H. (2009). *The elements of statistical learning: data mining, inference, and prediction*. Springer series in statistics. Springer, New York, NY, 2nd ed edition.
- Hotelling, H. (1933). Analysis of a complex of statistical variables into principal components. *Journal of Educational Psychology*, **24**, 498–520.
- Jacobi, C. (1834). De binis quibuslibet functionibus homogeneis secundi ordinis per substitutiones lineares in alias binas transformandis, quae solis quadratis variabilium constant; una cum variis theorematis de transformatione et determinatione integralium multiplicium. *Journal für die reine und angewandte Mathematik (Crelles Journal)*, pages 1 – 69.
- Johnstone, I. M. and Lu, A. Y. (2009). On consistency and sparsity for principal components analysis in high dimensions. *Journal of the American Statistical Association*, **104**(486), 682–693.
- Jolliffe, I. (2002). *Principal Component Analysis*. Springer Series in Statistics. Springer, New York, NY.
- Jolliffe, I., Trendafilov, N., and Uddin, M. (2003). A modified principal component technique based on the LASSO. *Journal of Computational and Graphical Statistics*, **12**(3), 531–547.
- Jolliffe, I. T. and Cadima, J. (2016). Principal component analysis: a review and recent developments. *Philos Trans A Math Phys Eng Sci*, **374**(2065), 20150202.
- Jung, S., Ahn, J., and Jeon, Y. (2019). Penalized orthogonal iteration for sparse estimation of generalized eigenvalue problem. *Journal of Computational and Graphical Statistics*, **28**(3), 710–721.
- Kluger, Y., Basri, R., Chang, J. T., and Gerstein, M. (2003). Spectral biclustering of microarray data: Coclustering genes and conditions. *Genome Research*, **13**(4), 703–716.
- Lu, J., Kerns, R. T., Peddada, S. D., and Bushel, P. R. (2011). Principal component analysis-based filtering improves detection for affymetrix gene expression arrays. *Nucleic Acids Research*, **39**(13), e86.
- Ma, S. and Dai, Y. (2011). Principal component analysis based methods in bioinformatics studies. *Briefings in Bioinformatics*, **12**(6, SI), 714–722.
- Ma, Z. (2013). Sparse principal component analysis and iterative thresholding. *Ann. Statist.*, **41**(2), 772–801.
- McInnes, L., Healy, J., and Melville, J. (2018). Umap: Uniform manifold approximation and projection for dimension reduction.
- Moghaddam, B., Weiss, Y., and Avidan, S. (2006). Spectral bounds for sparse pca: Exact and greedy algorithms. *Advances in neural information processing systems*, **18**, 915.
- Patterson, N., Price, A. L., and Reich, D. (2006). Population structure and eigenanalysis. *PLOS Genetics*, **2**(12), e190.
- Pearson, K. (1901). On lines and planes of closest fit to systems of points in space. *Philosophical Magazine*, **2**(6), 559–572.

- Ritchie, M. E., Phipson, B., Wu, D., Hu, Y., Law, C. W., Shi, W., and Smyth, G. K. (2015). limma powers differential expression analyses for rna-sequencing and microarray studies. *Nucleic Acids Res*, **43**(7), e47.
- Seurat (2020). Seurat guided clustering tutorial. https://satijalab.org/seurat/v3.1/pbmc3k_tutorial.html. Accessed: 2020-02-10.
- Shen, H. and Huang, J. Z. (2008). Sparse principal component analysis via regularized low rank matrix approximation. *Journal of Multivariate Analysis*, **99**(6), 1015–1034.
- Sriperumbudur, B. K., Torres, D. A., and Lanckriet, G. R. G. (2011). A majorization-minimization approach to the sparse generalized eigenvalue problem. *Machine Learning*, **85**(1-2), 3–39.
- Stuart, T., Butler, A., Hoffman, P., Hafemeister, C., Papalexi, E., Mauck, 3rd, W. M., Hao, Y., Stoeckius, M., Smibert, P., and Satija, R. (2019). Comprehensive integration of single-cell data. *Cell*, **177**(7), 1888–1902.e21.
- Tan, K. M., Wang, Z., Liu, H., and Zhang, T. (2018). Sparse generalized eigenvalue problem: optimal statistical rates via truncated rayleigh flow. *Journal of the Royal Statistical Society: Series B (Statistical Methodology)*, **80**(5), 1057–1086.
- Tanay, A. and Regev, A. (2017). Scaling single-cell genomics from phenomenology to mechanism. *Nature*, **541**(7637), 331–338.
- Tibshirani, R. (2011). Regression shrinkage and selection via the lasso: a retrospective. *Journal of the Royal Statistical Society. Series B (Statistical Methodology)*, **73**(Part 3), 273–282.
- Tomfohr, J., Lu, J., and Kepler, T. B. (2005). Pathway level analysis of gene expression using singular value decomposition. *BMC Bioinformatics*, **6**, 225.
- Vines, S. (2000). Simple principal components. *Journal of the Royal Statistical Society. Series C (Applied Statistics)*, **49**(Part 4), 441–451.
- Wagner, A., Regev, A., and Yosef, N. (2016). Revealing the vectors of cellular identity with single-cell genomics. *Nat Biotechnol*, **34**(11), 1145–1160.
- Waltman, L. and van Eck, N. J. (2013). A smart local moving algorithm for large-scale modularity-based community detection. *The European Physical Journal B*, **86**(11).
- Witten, D. M., Tibshirani, R., and Hastie, T. (2009). A penalized matrix decomposition, with applications to sparse principal components and canonical correlation analysis. *Biostatistics*, **10**(3), 515–534.
- Young, M. D., Wakefield, M. J., Smyth, G. K., and Oshlack, A. (2010). Gene ontology analysis for rna-seq: accounting for selection bias. *Genome Biol*, **11**(2), R14.
- Yuan, X.-T. and Zhang, T. (2013). Truncated power method for sparse eigenvalue problems. *J. Mach. Learn. Res.*, **14**(1), 899–925.
- Zou, H., Hastie, T., and Tibshirani, R. (2006). Sparse principal component analysis. *Journal of Computational and Graphical Statistics*, **15**(2), 265–286.